ELSEVIER

Chemical Engineering Journal 68 (1997) 173–187

Chemical Engineering Journal

Mechanism and kinetic control of the oxyprecipitation of sulphuric liquors from steel pickling

J. Dufour [a,b,*], J.O. Marrón [a,b], C. Negro [a], R. Latorre [a], A. Formoso [b], F. López-Mateos [a]

[a] *Chemical Engineering Department, Complutense University of Madrid, Madrid, Spain*

[b] *Primary Metallurgy and Materials Recycling Department, National Centre for Metallurgical Research (CSIC), Spain*

Received 10 January 1997; accepted 24 July 1997

Abstract

Steel pickling liquors are one of the main environmental problems of steel making. Currently, there are several processes for the treatment of sulphuric liquors, although most recover only acid and haematite (α-Fe_2O_3). We propose an oxyprecipitation process for this recovery, allowing several kinds of iron oxide or oxyhydroxide to be obtained. The aim of this paper is to determine the kinetic control and reaction mechanism. The influence of different variables is evaluated and two experimental ranges for the synthesis of goethite (α-FeOOH) and magnetite (Fe_3O_4) are defined. A systematic study is carried out in these experimental intervals, and the results are analysed in order to determine the reaction order and the type of kinetic control. Finally, from these data, morphological and crystallinity studies and new experiments, the reaction mechanism is proposed. © 1997 Elsevier Science S.A.

Keywords: Mechanism; Kinetics; Oxidation; Precipitation; Iron oxides

1. Introduction

The pickling process is used for the surface treatment of steel slabs and involves the dissolution of the superficial layers of iron oxides formed during the steel making process. It is carried out by submerging the slabs in sulphuric or hydrochloric acid baths. Subsequently, the slabs are rinsed in order to remove traces of acid and dissolved iron. The discharge of the generated wastes (spent pickling liquors) is the main source of water pollution in the steel making industry.

Currently, several processes are available for the treatment of hydrochloric liquors [1]; however, the treatment of sulphuric liquors yields problems associated with the recovery of dissolved Fe(II). The crystallization of copperas [2] was a useful method but has been affected by the saturation of the market. The electrolytic deposition of Fe^0 [3] is too expensive in many countries. Acid retardation [4] generates a ferrous sludge with poor recovery and low price. The use of monopolar or bipolar membranes requires dilute solutions (pickling liquors are very concentrated) or the previous precipitation of dissolved Fe(II) [5]. Roasting [6] produces only α-Fe_2O_3 as a final product, often with a broad size distribution. Finally, solvent extraction [7] and bio-oxidation [8] exhibit slow kinetics and, therefore, require large reaction times.

We propose an oxyprecipitation process for the large-scale treatment of pickling liquors. Oxyprecipitation is a form of treatment used on waste liquors such that, when suitable chemicals (bases and oxidizing agents) are added, it is possible to alter the physical state of the dissolved or suspended solids to facilitate their elimination through a sedimentation process. In this way, it is possible to obtain iron oxides and oxyhydroxides (α-Fe_2O_3, α-FeOOH, Fe_3O_4, γ-FeOOH, etc.) from the high iron concentration of these liquors.

Much research has been published on the reaction mechanisms of precipitation of these oxides. In this paper, we revise the mechanisms concerning the nucleation of α-FeOOH and Fe_3O_4.

1.1. Goethite

This oxide may be obtained in strongly alkaline solutions or by the addition of OH^- to acidic solutions [9]. In alkaline solution, the mechanism is:

$$Fe(OH)_2 \rightarrow Fe(OH)_3^- \rightarrow Fe(OH)_3 \rightarrow FeO_x(OH)_{3-2x} \rightarrow \alpha\text{-FeOOH} \quad (1)$$

* Corresponding author. Chemical Engineering Department, Fac. Chemical Sciences, Complutense University of Madrid, Avda. Complutense s/n. 28008 Madrid, Spain. Tel.: +34-1-3944247; fax: +34-1-3944114; e-mail: dufour@eucmax.sim.ucm.es

PII S1385-8947(97)00093-4

This mechanism begins with the formation of $Fe(OH)_3^-$ ($HFeO_2^-$) by the dissolution of $Fe(OH)_2$ in alkaline conditions. It is then oxidized to electroneutral $Fe(OH)_3$, which is polymerized to colloidal $[Fe(OH)_3]_n$. Finally, this compound precipitates as ferrihydrite ($FeO_x(OH)_{3-2x}$, amorphous oxyhydroxide) by dehydration followed by rapid conversion into α-FeOOH.

This reaction scheme was also explained by Kiyama [10], and Sada et al. [11] in the form of polycations

$$HFeO_2^- + O_2 \rightarrow [Fe_2(OH)_3^{3+}] \xrightarrow{\text{polymerization}} [Fe_2(OH)_3]_n^{3+} \quad (2)$$

$$[Fe_2(OH)_3]_n^{3+} + H_2O \rightarrow \alpha\text{-FeOOH} \quad (3)$$

In acidic solutions, Misawa et al. [9] proposed the mechanism

$$\begin{array}{l} \qquad\qquad\quad Fe^{3+} \\ \qquad\qquad\quad \downarrow OH^- \\ \xrightarrow{O_2} \quad \xrightarrow{Fe^{3+}+OH^-} \qquad\qquad\quad \xrightarrow{OH^-} \\ FeOH^+ \rightarrow Fe(OH)_2^+ \rightarrow [Fe(OH)_{3-x}^{x+}]_n \rightarrow FeO_x(OH)_{3-2x} \rightarrow \alpha\text{-FeOOH} \\ \uparrow \qquad\qquad\qquad\qquad\qquad\qquad\qquad\qquad\qquad\qquad \uparrow \\ Fe^{2+} \rightarrow Fe(II)_1O_xFe(III)_3^{(11-2x)+} \text{———————} \end{array} \quad (4)$$

Goethite is obtained by the conversion of ferrihydrite, formed by the precipitation of the intermediate polycation via polymerization of $Fe(OH)_2^+$. The latter may be obtained by the oxidation of $FeOH^+$ (soluble phase of $Fe(OH)_2$) or by the hydrolysis of Fe^{3+} promoted by the addition of OH^-.

In addition, ferrihydrite can be precipitated by the oxidation and neutralization of green complex II (G.C. II) from strongly acidic solutions. The G.C. II is nucleated during the air oxidation of ferrous sulphate in slightly alkaline conditions, followed by the precipitation of green rust II (G.R. II) [12]. In later research on the oxidation of $FeSO_4$ solution at pH 6.8 [13], it was observed that the Fe(II)/Fe(III) molar ratio in the G.C. II structure was 2:1. The transformation of ferrihydrite to goethite in acidic conditions requires very large reaction times (several years may be necessary).

Detournay et al. [14] proposed a different mechanism involving two steps: oxidation of $Fe(OH)_2$ to G.R. II ($2Fe(OH)_3 \cdot 4Fe(OH)_2 \cdot FeSO_4 \cdot xH_2O$) and transformation into α-FeOOH. The formula of G.R. II was refined to ($4Fe(OH)_2 \cdot 2FeOOH \cdot FeSO_4 \cdot 4H_2O$) using Mössbauer spectroscopy [15].

A final reaction scheme involves the nucleation of goethite from the dissolution of lepidocrocite (γ-FeOOH) by heating $FeSO_4$ solutions.

1.2. Magnetite

The first mechanism begins with the formation of green rusts or green complexes and their transformation into Fe_3O_4 by slow oxidation in mild pH conditions. If the oxidation is rapid, the final product is γ-FeOOH. The reaction schemes are [9]

$$Fe(OH)_2 \xrightarrow{O_2} \text{G.R.II} \begin{cases} \xrightarrow{O_2\downarrow} Fe_3O_4 \\ \xrightarrow{O_2\uparrow} \gamma\text{-FeOOH} \end{cases} \quad (5)$$

$$Fe(OH)_2 \xrightarrow{O_2} \text{G.C.II} \begin{cases} \xrightarrow{O_2\downarrow} Fe_3O_4 \\ \xrightarrow{O_2\uparrow} \gamma\text{-FeOOH} \end{cases} \quad (6)$$

These mechanisms are based on the difficult conversion of ferrous hydroxide with hexagonal structure to magnetite or lepidocrocite, both with a cubic structure. During the nucleation of magnetite, two oxygen ions must be extracted for every three molecules of ferrous hydroxide. If the oxidation is carried out slowly, the time for oxygen extraction from the crystal and for rearrangement of the remaining iron and oxygen will be sufficient for the formation of magnetite; however, if the reaction is fast, rearrangement will not be possible, promoting the nucleation of lepidocrocite. This oxyhydroxide can be spontaneously transformed into magnetite when sulphate ions are present [16].

The second mechanism begins with the precipitation and dehydration of the red complex cation $[Fe(II)_1Fe(III)_2O_x(OH)_{2(3-x)}]_{2m}^{2m+}$. In solutions in which the Fe(II)/Fe(III) molar ratio is 1:2 or higher, the precipitation will not occur until pH 7. This intermediate may also be formed by the addition of OH^- to green complex solutions.

$$m\text{Fe(II)} + 2m\text{Fe(III)} + 6m(OH)^- \rightarrow [Fe(II)_1Fe(III)_2)O_x(OH)_{2(3-x)}]_{2m}^{2m+} + mxH_2O \quad (7)$$

$$[Fe(II)_1Fe(III)_2)O_x(OH)_{2(3-x)}]_{2m}^{2m+} + 2mOH^- \rightarrow mFe_3O_4 + (4-x)mH_2O \quad (8)$$

At higher pH, the mechanism can be explained as a slow coprecipitation of $FeOH^+$ with hydroxoferric complexes [10]. In these conditions, the nuclei of $Fe(OH)_2$ or green rust are enclosed in a dense layer of $FeOH^+$, where coprecipitation occurs. The reaction begins with the oxidation of the cation by dissolved oxygen [11]

$$2FeOH^+ + \frac{1}{2}O_2 + H_2O \rightarrow [Fe_2(OH)_3]^{3+} + OH^- \quad (9)$$

This ferric ion coprecipitates with ferrous ion to produce magnetite

$$[Fe_2(OH)_3]^{3+} + FeOH^+ + 4OH^- \rightarrow Fe_3O_4 + 4H_2O \quad (10)$$

The latter reaction can be understood as

$$[Fe_2(OH)_3]^{3+} + FeOH^+ + 2OH^- \rightarrow Fe_3O(OH)_4^{2+} + H_2O \quad (11)$$

$$Fe_3O(OH)_4^{2+} + 2OH^- \rightarrow Fe_3O_4 + 3H_2O \quad (12)$$

$Fe_3O(OH)_4^{2+}$ agrees with the formula of the red complex cation when $x = 1$.

Other complex intermediates with different stoichiometries have been proposed, but magnetite is always formed from an intermediate containing the same Fe^{2+}/Fe^{3+} ratio [17].

2. Materials and methods

The studied ranges and variables were as follows: pH 3–8; stirring speed, 0–1000 rpm; two oxidizers, air and oxygen, 99.5%; flow of oxidizer, 5–20 l min^{-1}; and temperature, 298–343 K.

Sulphuric pickling liquors were used as raw materials. They were collected on the rolling mills of Ensidesa (Avilés, Spain), with Fe(II) concentrations between 35 and 55 g l^{-1} and free acid between 8% and 12%. Ammonium hydroxide (reagent grade) was chosen as basic agent.

The experimental equipment and procedure have been described previously [18]. During the previous experiments, the reactions were completed at 180 min for 298 and 318 K and at 90 min for 343 K, or when the Fe(II) was exhausted. During the systematic study, periodic sampling was performed, the experiments were stopped when the Fe(II) was exhausted or when the pH variation was very slow, indicating the long duration of the experiment.

The X-ray diffraction (XRD) intensities of the characteristic peaks of goethite and magnetite (corresponding to $d_{110}=4.18$ Å and $d_{311}=2.53$ Å, respectively) [19], corrected by the external or internal standard method using tungsten, and the Fe(II) elimination rate were selected as quality parameters.

A Siemens Kristalloflex 810 goniometer with Cu Kα radiation (Ni filter) with computerized data collection back-up was used for XRD. For scanning electron microscopy (SEM), a JEOL JSM-6400 microscope was used.

Table 1
Fe(II) elimination vs. pH

Fixed conditions: $N=750$ rpm, $Q_a=10$ l min^{-1}

T (K)	pH	$Cm_{Fe(II)0}$ (g/l)	$Cm_{Fe(II)f}$ (g/l)	$Cm_{Fe(III)f}$ (g/l)	$\%Fe_{el}$	t (min)
298	4	45.50	28.96	0.12	25.0	180
	5	39.13	1.21	–	96.2	170
	6	46.83	0.08	–	99.9	90
	7	46.20	0.28	0.02	99.8	85
318	3	45.12	29.26	0.42	35.0	180
	4	47.05	21.15	0.38	55.0	180
	5	48.18	5.88	0.14	88.0	180
	6	44.80	0.05	–	98.0	60
	7	38.86	0.22	–	99.4	45
343	3	44.23	29.41	0.89	33.5	90
	4	57.80	33.32	0.46	42.3	90
	5	42.22	6.75	0.21	84.0	90
	6	41.88	0.84	–	98.0	90
	7	37.90	0.22	–	99.4	90
	8	43.15	0.34	–	99.2	90

3. Previous experiments: Selection of experimental ranges for systematic study

3.1. Study of pH

Fig. 1 and Table 1 show the results obtained as a function of pH. Goethite is the only product at 298 K and pH 4, 5 or 6. At pH 7, a mixture of goethite and magnetite is obtained. In all cases, the synthesized α-FeOOH presents low crystallinity. In Fig. 2, it can be seen that the product formed is composed of very heterogeneous, broad particles; this does not agree with the acicular morphology of goethite. However, from Fig. 3, where two micrographs at different magnifications are presented, we can see an incipient growth of needle-like particles over the surface of the broad particle.

At higher temperatures (318 and 343 K), a similar behaviour is observed; the maximum crystallinity is obtained at pH 4, being slightly higher at $T=318$ K. However, the mixtures are obtained at lower pH values (pH 6 at 318 K and pH 5 at

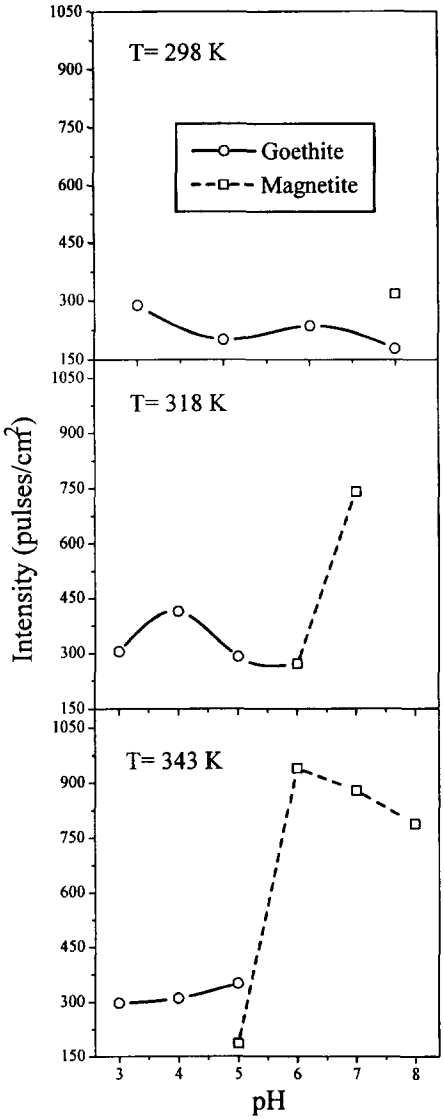

Fig. 1. Plot of the XRD intensity of the characteristic peaks of goethite and magnetite vs. pH.

Fig. 2. Micrographs of products synthesized as a function of pH (T=298 K): (a) pH 4; (b) pH 5; (c) pH 6.

343 K), indicating that temperature promotes the synthesis of magnetite.

Above 343 K and pH 7, the magnetite exhibits less crystallinity, due to the formation of numerous crystallization nuclei, and, therefore, smaller particles are obtained (Fig. 4).

The presence of basic sulphates [20] in the final products was detected by XRD. This fact was corroborated by X-ray fluorescence (XRF) analysis, summarized in Table 2. An anomalously high concentration of sulphur can be seen in the product precipitated at pH 4 and 298 K.

3.2. Study of stirring speed

The results obtained are presented in Fig. 5 and Table 3. Very different behaviour is observed at the lower temperatures and at 343 K, probably due to two competing reactions for the synthesis of magnetite and goethite at these temperatures.

An inflexion in the crystallinity is observed at 750 rpm at 298 K and at 500 rpm at 318 K. This effect is due to two opposing factors: on the one hand, the increase in stirring speed provokes higher turbulence in the reactive medium, inhibiting the formation of crystallization nuclei; on the other, the increase in stirring speed promotes the oxygen diffusion rate which improves the oxidation of Fe(II) [21] and the nucleation of goethite.

At 343 K, magnetite is obtained in the experiments performed without stirring and at the highest stirring speeds. Three effects should be borne in mind: goethite has a larger particle size than magnetite and requires a stable medium for nucleation; as explained previously, high speeds improve Fe(II) oxidation and, therefore, inhibit the nucleation of magnetite; finally, high temperature promotes the synthesis of magnetite. Thus, the best magnetite is obtained at 0 rpm, because the oxygen diffusion is very poor. On increasing the stirring speed to 250 or 500 rpm, Fe_3O_4 is not nucleated because the medium is not sufficiently turbulent, and the nucleation of α-FeOOH occurs. At higher stirring speeds (higher turbulence), magnetite of smaller size is synthesized.

3.3. Study of air flow

Fig. 6 and Table 4 show the results obtained as a function of air flow. A very different behaviour is again observed at 343 K.

The trend in α-FeOOH crystallinity is analogous for the two lower temperatures. It increases as the air flow increases due to the improved Fe(II) oxidation, achieving a maximum at 15 l min^{-1}. At 20 l min^{-1}, the peak intensity decreases probably due to the higher turbulence, high ascending velocity of oxidizer bubbles and low solubility of oxygen in acidic solutions which inhibit goethite crystallization.

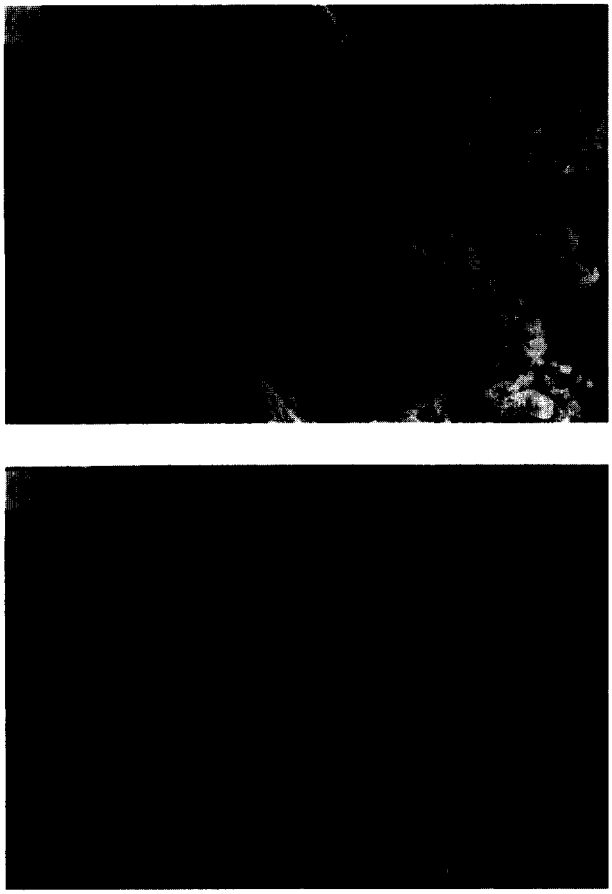

Fig. 3. Micrographs of the product synthesized at $T = 298$ K and pH 4.

At 343 K, goethite and magnetite are obtained, showing the competitive nature of their formation reactions. Magnetite is nucleated at lower air flows, because oxidation is slower, preventing the complete oxidation of previously precipitated Fe(II). When the air flow is increased, oxidation is enhanced yielding goethite and inhibiting magnetite nucleation, which is totally depressed at 15 l min^{-1}.

3.4. Study of oxygen flow

Again, a very different behaviour is observed between the experiments carried out at 343 K and at lower temperatures (Fig. 7). Table 5 shows the Fe(II) elimination for this series of experiments. The 298 and 318 K isotherms show that the maximum crystallinity is achieved at 5 l min^{-1}, due to the high oxygen concentration and low turbulence, which allow a better nucleation of goethite.

The minimum value is obtained at 10 l min^{-1}, because precipitation occurs instantaneously, but the flow is insufficient to achieve oxidation in the solid state. When the flow is increased to 15 l min^{-1}, the crystallinity is improved due to the total oxidation of the solid.

Magnetite is obtained in all the experiments carried out at 343 K. This phenomenon may be explained by the fast precipitation of dissolved iron and by the higher temperature which promotes the nucleation of Fe_3O_4.

The products obtained at 298 and 318 K using air or oxygen are very similar, but the use of air at 343 K produces oxides of higher crystallinity due to the longer reaction times which allow the growth of nuclei. However, it is necessary to work at higher air flows than oxygen flows ($Q_a = 15$ l min^{-1} vs. $Q_o = 10$ l min^{-1}).

3.5. Fe(II) elimination

From Tables 1, 3–5, it can be seen that high Fe(II) eliminations are not achieved when the experiments are carried out at pH < 5. At higher pH values, total elimination is obtained at short reaction times. In general, an increase in all the variables improves the Fe(II) elimination rate, in particular pH and temperature. Stirring improves the diffusion of oxygen and therefore oxidation, accelerating the elimination speed. In the same way, an increase in flow or the use of oxygen exert a similar effect.

4. Systematic study

4.1. Selection of experimental ranges for systematic study

With the aim of determining the reaction mechanism and kinetic control, two experimental ranges were defined: one for the synthesis of goethite and one for the nucleation of magnetite, both as pure phases (Table 6).

For the synthesis of goethite, the chosen pH interval was pH 3.5–4.5, because it ensured the formation of α-FeOOH. Lower pH values promote the nucleation of heterogeneous particles and higher pH values promote the synthesis of magnetite. Although air and $T = 318$ K were also studied, oxygen as oxidizer and 343 K as the working temperature were found to be the optimum parameters due to their increasing effect on Fe(II) oxidation. The stirring speed was chosen between 500 and 1000 rpm, because lower speeds inhibit oxygen diffusion and higher velocities promote the nucleation of magnetite. Finally, the flow was studied between 10 and 20 l min^{-1}, allowing slow or fast oxidation.

For the synthesis of magnetite, a temperature of 343 K was selected as it led to an improvement in magnetite nucleation (a few experiments were carried out at 318 K to study the kinetics). The chosen pH interval was pH 5.5–6.5, because mixtures of goethite and magnetite are obtained at lower values and the crystallinity decreases at higher values. Air with a flow between 5 and 10 l min^{-1} was chosen as the oxidizer, because the use of oxygen or higher flows promotes the synthesis of goethite. The stirring speed range was 250–1000 rpm, because heterogeneous experiments occur at lower speeds, preventing control.

Some experiments were performed outside these experimental ranges in order to develop two mathematical models for the synthesis of goethite [18] and magnetite [22]. Thus 55 experiments were carried out. Figs. 8–10 show representative examples of the results obtained.

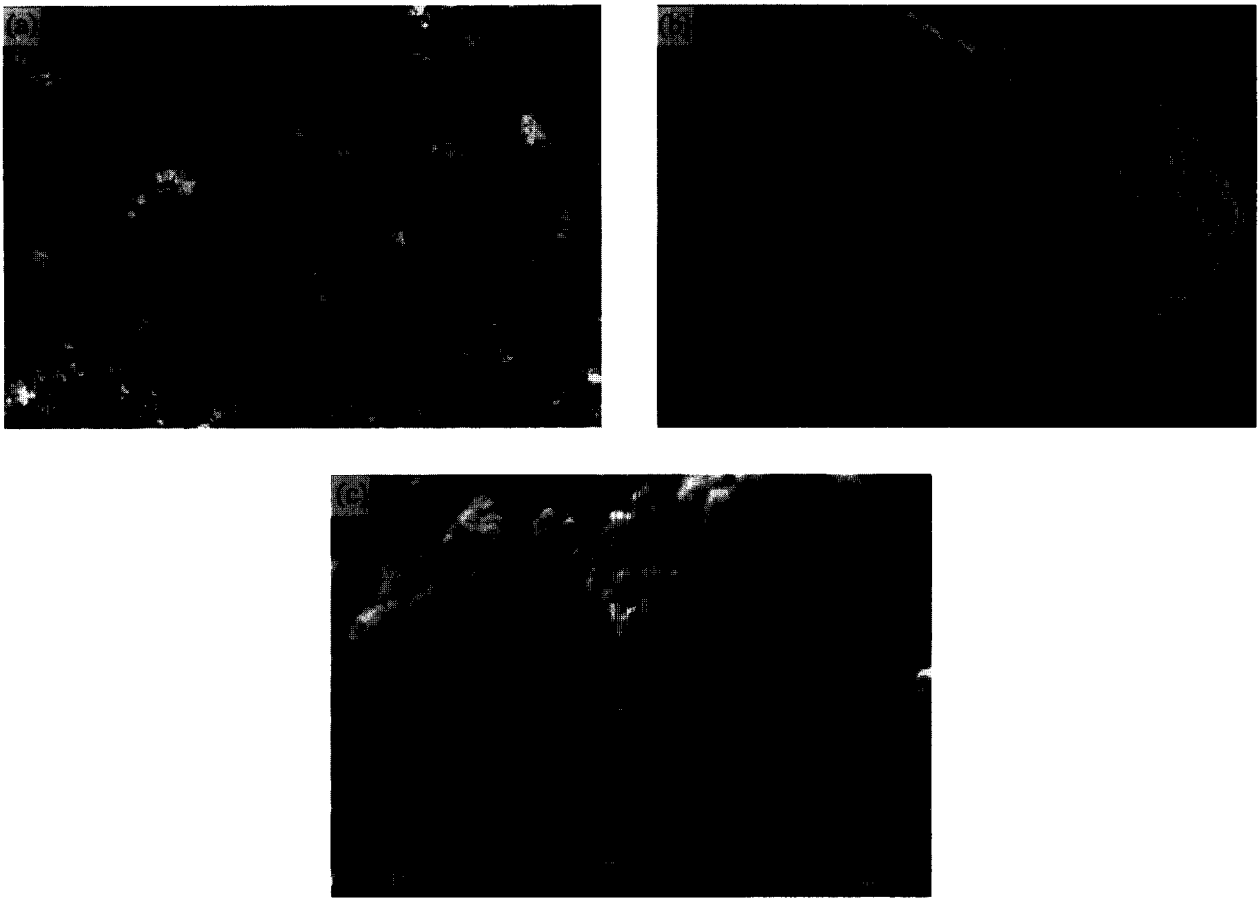

Fig. 4. Micrographs of products synthesized as a function of pH (T=343 K): (a) pH 6; (b) pH 7; (c) pH 8.

5. Kinetic control

The slopes of the plotted Fe(II) elimination curves vary as a function of pH. At pH ≥ 5.5, curves with a sharp initial slope are obtained. Later, the slope flattens out until total Fe(II) elimination is achieved. At lower pH values, smooth curves are obtained. These observations suggest that two mechanisms occur.

Oxidation of Fe(II) in the liquid phase, followed by the rapid precipitation of oxyhydroxide, occurs at low pH values (pH 3–5)

$$Fe^{2+}_{(d)} \rightarrow Fe^{3+}_{(d)} \rightarrow Fe^{3+}_{(s)} \quad (13)$$

Table 2
Microanalysis of products

Experimental conditions				Microanalysis		
N (rpm)	Q_a (l min^{-1})	T (K)	pH	Fe (%)	S (%)	O (%)
750	10	25	4	12.35	5.14	82.51
			7	18.95	1.04	80.01
		45	6	17.08	1.05	81.87
		70	4	15.82	1.52	82.66
			8	18.89	0.55	80.56

The second mechanism takes place at higher pH values (pH 5–8). It involves the rapid precipitation of $Fe(OH)_2$ from part of the dissolved Fe(II) and its oxidation in the solid state. The remaining dissolved Fe(II) is oxidized as in Eq. (13)

$$Fe(II)_{(d)} \begin{cases} \rightarrow Fe(II)_{(s)} \rightarrow Fe(III)_{(s)} \\ \rightarrow Fe(III)_{(d)} \rightarrow Fe(III)_{(s)} \end{cases} \quad (14)$$

The latter mechanism explains the sharp slope and is kinetically controlled by the oxidation of dissolved Fe(II) to dissolved Fe(III), because precipitation occurs rapidly. Therefore the study of the kinetic control of oxyprecipitation can be reduced to the investigation of the Fe(II) to Fe(III) oxidation in the liquid phase, which is a two-phase gas–liquid system, where oxygen acts as the oxidizer and the pickling liquor as the oxidizable liquid. The oxidation reaction is given by the following expression

$$4Fe(II)_{(d)} + 4H_3O^+_{(d)} + O_{2(g)} \rightarrow 4Fe(III)_{(d)} + 6H_2O_{(d)}. \quad (15)$$

In order to determine the type of control, it is necessary to carry out a comparative study between the speed of the chemical reaction and the speed of oxygen diffusion. Depending

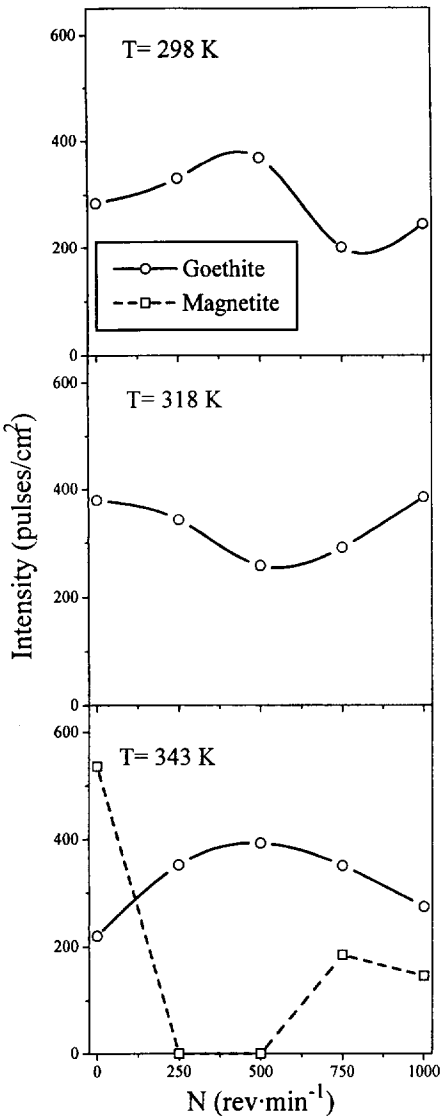

Fig. 5. Plot of the XRD intensity of the characteristic peaks of goethite and magnetite vs. the stirring speed.

on the stage which exerts control, the following kinetic equations are obtained.

5.1. Chemical control

$$(-r_{O_2}) = \frac{(-r_{Fe(II)})}{4} = -\frac{1}{4}\frac{dFe(II)}{dt} = Kp_{O_2}^{n} C_{Fe(II)}^{m} \qquad (16)$$

Assuming that the reaction is first-order with respect to oxygen and that its partial pressure remains constant during the experiments due to the high flows used, the following expressions are obtained by integration between the limit conditions of the system $m = 1$

$$\ln C_{Fe(II)} = \ln C_{Fe(II)0} - 4Kp_{O_2}t \qquad (17)$$

$m \neq 1$

$$C_{Fe(II)}^{(1-m)} = C_{Fe(II)0}^{(1-m)} - (m-1)4Kp_{O_2}t \qquad (18)$$

5.2. Diffusional control

$$(-r_{O_2})\frac{(-r_{Fe(II)})}{4} = -\frac{1}{4}\frac{dFe(II)}{dt} = S\frac{\frac{D_{Fe(II)}}{4D_{O_2}}C_{Fe(II)} + \frac{p_{O_2}}{H_{O_2}}}{\frac{1}{H_{O_2}K_{O_2g}} + 1\frac{O}{K_{O_2l}}} \qquad (19)$$

The resistance in the gas phase can be considered to be negligible ($K_{O_2g} = \infty$), because the solubility of oxygen in water solutions is low, especially at low pH, and the partial pressure of oxygen can be considered to be high. Integrating between the limit conditions, Eq. (20) is obtained

$$\ln(WC_{Fe(II)}) = \ln(WC_{Fe(II)0}) - \left(\frac{D_{O_2l}}{D_{Fe(II)}}\right)K_{O_2l}St \qquad (20)$$

where $W = D_{Fe(II)}/4D_{O_2l}$ and $Z = P_{O_2}/H_{O_2}$.

Tables 7 and 8 summarize the results of the analysis of the experimental data up to 98% Fe(II) elimination for chemical reaction control up to third-order (Eqs. (17) and (18)) and for diffusion control (Eq. (20)). At pH 3.5, the reaction corresponds to an order higher than unity. When air is used as an oxidizer, the best correlations are obtained for a third-order model, but when the oxidation is improved by the use of oxygen, a second-order model provides better indices. This suggests that the kinetics show a complex mechanism or an equilibrium model.

At pH 4, similar correlations are obtained for first- and second order at 318 K in air, but when the temperature is increased to 343 K or oxygen is used, only the first-order model fits the data. However, these values are very similar to the correlation indices obtained for diffusion control. A slight trend to diffusion control is observed when the experiments are carried out at pH 4.5 and pH 4.8. On the other hand, the chemical reaction is first order.

In the pH range 3.5–4.8, the final product is goethite, showing higher crystallinity at higher pH or temperature.

At pH 5.2, a small amount of magnetite is synthesized in a mixture with goethite; its kinetic control corresponds to a shared model between diffusion and first-order reaction.

Magnetite is obtained as the only phase in the second experimental range. The experiments carried out at 318 K show second-order kinetic control, but a slight trend to diffusion control is obtained when the temperature is increased to 343 K and the chemical reaction is first order with respect to Fe(II) at all pH values.

Tables 9 and 10 show the calculated kinetic constants for the experiments with a first-order model. It can be seen that the reactions occurring at pH 3.5–4.5 show lower constants (most between 1.5×10^{-3} and 7.5×10^{-3}) than those in the higher pH interval (pH 5.5–6.8) (constants between 2.2×10^{-2} and 4.1×10^{-2}), demonstrating the different types of reaction. The experiments at intermediate pH values (pH 4.8 and pH 5.2) show intermediate constants.

Table 3
Fe(II) elimination vs. stirring speed

Fixed conditions: pH 5, $Q_a = 10\ l\ min^{-1}$

T (K)	N (rpm)	$Cm_{Fe(II)0}$ (g/l)	$Cm_{Fe(II)f}$ (g/l)	$Cm_{Fe(III)f}$ (g/l)	%Fe_{el}	t (min)
298	0	46.61	9.38	0.24	80.0	180
	250	48.03	18.99	0.21	60.5	180
	500	47.55	19.13	0.31	60.0	180
	750	39.13	1.21	–	96.9	170
	1000	36.60	8.62	0.14	76.4	180
318	0	39.00	0.38	–	98.9	180
	250	39.91	0.11	–	99.7	125
	500	36.94	0.14	–	99.6	115
	750	48.18	5.88	0.42	88.9	180
	1000	37.72	0.38	–	99.0	85
343	0	55.99	15.90	0.31	71.6	90
	250	40.67	9.35	0.25	77.0	90
	500	40.14	7.41	0.36	82.2	9900
	750	42.22	6.75	0.42	84.0	90
	1000	39.62	5.44	0.21	86.3	90

Table 4
Fe(II) elimination vs. air flow

Fixed conditions: pH 5, $N = 1000$ rpm

T (K)	Q_a ($l\ min^{-1}$)	$Cm_{Fe(II)0}$ (g/l)	$Cm_{Fe(II)f}$ (g/l)	$Cm_{Fe(III)f}$ (g/l)	%Fe_{el}	t (min)
298	5	45.30	3.02	0.27	93.3	180
	10	36.60	8.62	0.14	76.4	180
	15	46.54	4.32	0.27	91.0	180
	20	47.12	1.27	0.08	98.0	180
318	5	45.35	–	–	99.9	165
	10	37.70	0.38	0.02	99.0	85
	15	47.73	0.27	–	99.4	135
	20	44.72	0.22	–	99.5	135
343	5	40.75	11.90	0.42	70.6	90
	10	39.62	5.44	0.21	86.3	90
	15	40.89	3.88	0.27	90.5	90
	20	45.98	3.23	0.18	93.0	90

These results indicate that oxyprecipitation in the goethite synthesis range shows shared kinetic control between diffusion and first-order reaction at pH > 4 and chemical control when the pH is lower or the oxidation conditions are poor. Two different reactions are also observed in the magnetite synthesis range: second-order reaction is the controlling stage at 318 K, but when the temperature is increased, the control is shared between diffusion and first-order reaction. Thus, four processes seem to take place in the experimental ranges.

6. Reaction mechanism

6.1. Goethite

In order to study the possible processes, several experiments were carried out, freezing them at fixed times. From the macroscopic point of view, the products obtained at pH 3–4 (when low temperature or air was used) were mixtures of a brown powder and a gelatiniform solid, which was transformed to α-FeOOH of low crystallinity by oxidation in an air oven. At pH 4, 4.5 or 4.8, only goethite was detected as the final product.

Fig. 11 shows the XRD pattern of a product synthesized at pH 3.0. A mixture of jarosite-type sulphates, goethite and a compound which fits the XRD data file for G.R. II was observed. The presence of this compound was not detected at pH values higher than pH 4, even at the shortest reaction times (2–10 min). These results are in accordance with those summarized in Table 2, which show a high concentration of sulphur in the product obtained at pH 4. The different kinds of products can be seen in Fig. 12, where three representative micrographs are presented. At the lowest pH, an amorphous hexagonal-like solid is obtained, whereas a well-defined solid

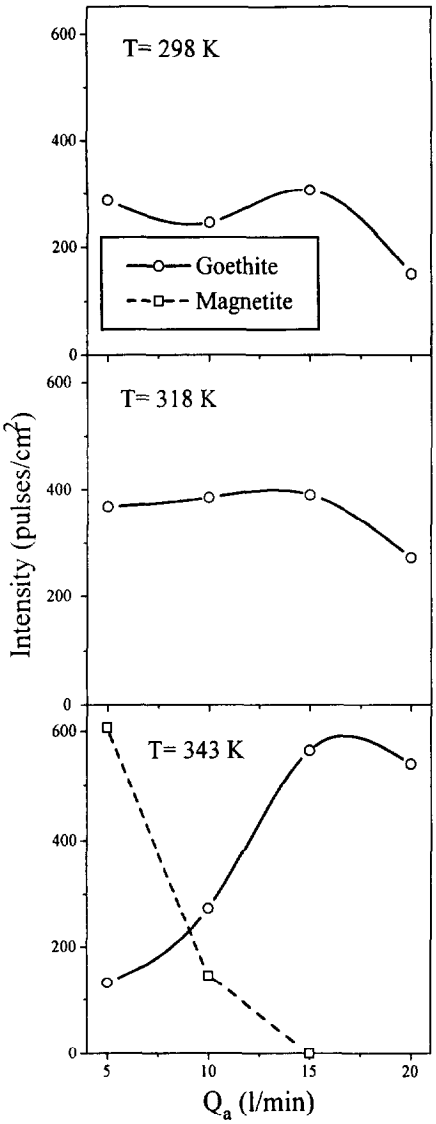

Fig. 6. Plot of XRD intensity of the characteristic peaks of goethite and magnetite vs. the flow of air.

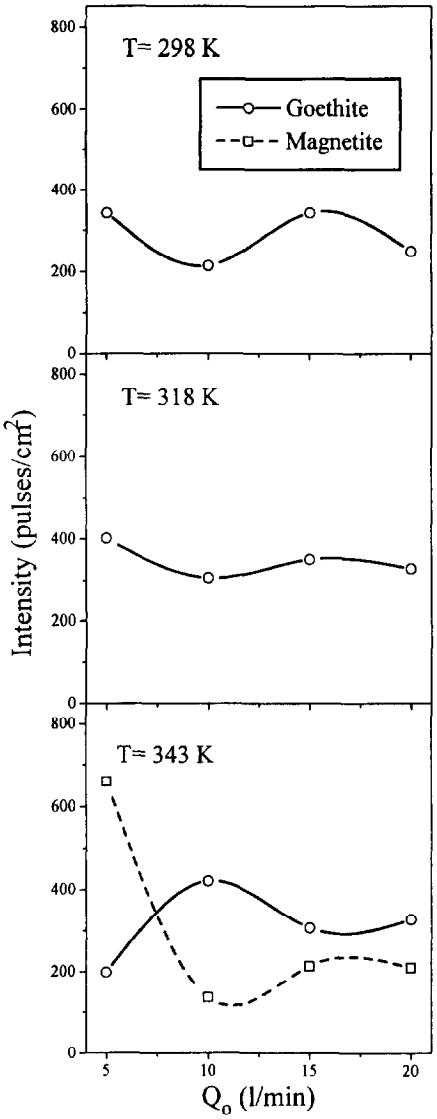

Fig. 7. Plot of the XRD intensity of the characteristic peaks of goethite and magnetite vs. the flow of oxygen.

is synthesized for the highest pH. The compounds proposed by other researchers as intermediates in the synthesis of goethite, ferrihydrite and lepidocrocite, were not detected at any of the tested experimental conditions.

These results indicate that the synthesis of goethite at pH 3.5 or pH 4, when the oxidation conditions are poor, requires the nucleation of G.R. II as an intermediate. It is very improbable that G.R. II is nucleated directly from Fe(II) solutions, and the most probable route is via the formation of G.C. II as an initial intermediate. The micrographs shown in Fig. 3 support this mechanism, because goethite is observed growing over amorphous particles with high sulphur concentration (Table 2). However, G.R. II is not formed at pH 4–4.8; therefore, G.C. II must be nucleated before the precipitation of α-FeOOH, due to the impossibility of the direct transformation of Fe(II) into goethite. This mechanism is confirmed by the correlations obtained in the kinetic control studies: the process is controlled by a complex or equilibrium reaction model at low pH, which is characteristic of reactions with more than one involved intermediate.

6.2. Magnetite

The mechanism for the nucleation of magnetite at 343 K begins with the rapid precipitation of part of the Fe(II) which can be observed macroscopically. The analysis of this solid shows that it is amorphous with Fe(II) as the main constituent, although a small amount of Fe(III) can be detected (approximately 1%). This suggests that the solid must be $Fe(OH)_2$, which is partially redissolved, $FeOH^+$ being the stable form. The latter cation reacts to nucleate an intermediate complex which precipitates as Fe_3O_4. This complex must have the same Fe(II)/Fe(III) ratio as magnetite, as discussed in Section 1. Probably, the formation of the inter-

Table 5
Fe(II) elimination vs. oxygen flow

Fixed conditions: pH 5, $N = 1000$ rpm

T (K)	Q_o (l min^{-1})	$Cm_{Fe(II)0}$ (g/l)	$Cm_{Fe(II)f}$ (g/l)	$Cm_{Fe(III)f}$ (g/l)	%Fe_{el}	t (min)
298	5	54.60	1.27	–	98.0	35
	10	46.69	0.14	–	99.7	25
	15	47.81	–	–	99.9	20
	20	47.73	0.14	–	99.7	23
318	5	43.49	0.11	0.21	99.7	27
	10	38.69	0.06	–	99.8	30
	15	39.13	0.14	–	99.6	20
	20	36.00	0.14	0.02	99.6	20
343	5	44.51	0.02	–	99.9	25
	10	53.35	0.21	–	99.6	30
	15	46.08	0.11	–	99.8	22
	20	41.82	0.11	–	99.8	25

Table 6
Experimental ranges for the systematic study of the synthesis of goethite and magnetite

Variable	Goethite	Magnetite
pH	3.5–4.5	5.5–6.5
Temperature (K)	318–343	318–343
Stirring speed (rpm)	500–1000	250–1000
Oxidizer	Air and O_2	Air
Flow (l/min)	10–20	5–10

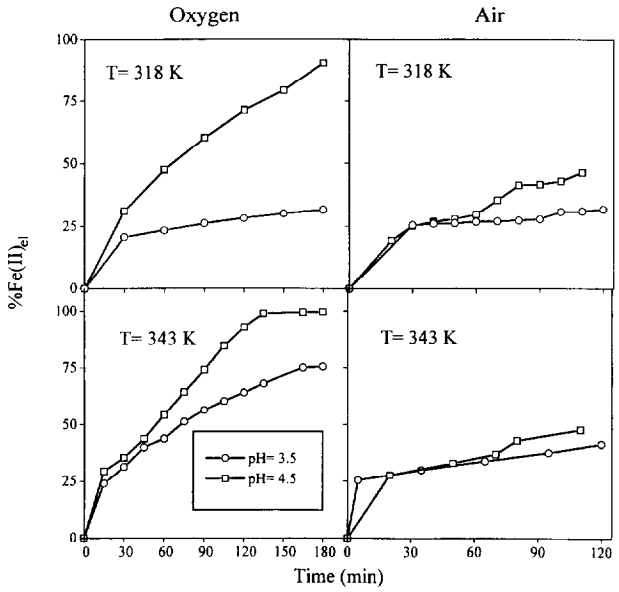

Fig. 8. Plot of Fe_{el} (%) obtained at $N = 500$ rpm and $Q = 10$ l min^{-1}.

mediate occurs over the surface of the precipitated $Fe(OH)_2$ particles (as proposed by Kiyama [10], although for higher pH values), producing a solid similar to that shown in Fig. 4, where several agglomerates growing over a broad layer can be seen.

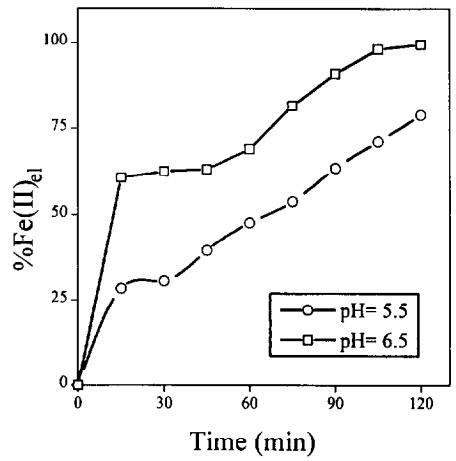

Fig. 9. Plot of Fe_{el} (%) obtained at $N = 250$ rpm, $Q_a = 5$ l min^{-1} and $T = 343$ K.

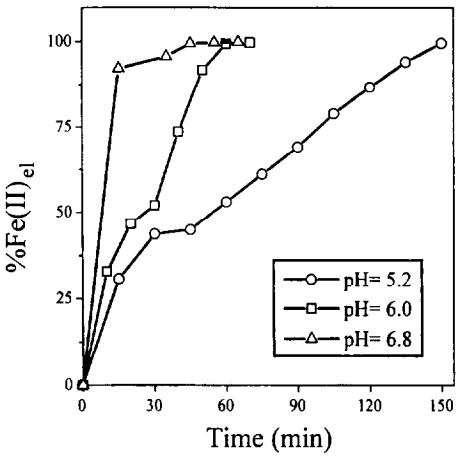

Fig. 10. Plot of Fe_{el} (%) obtained at $N = 625$ rpm, $Q_a = 7.5$ l min^{-1} and $T = 343$ K.

When the pH is fixed at intermediate values, mixtures of goethite and magnetite are obtained without the observation of precipitation. It is probable that the intermediate complex

Table 7
Correlation indices for chemical reaction of order one, two or three with respect to Fe(II) and diffusion of O_2. Goethite synthesis range

pH	T (K)	Oxidizer	N (rpm)	Q (l/min)	m=1	m=2	m=3	Diffusion
3.5	318	Air	500	10	0.878	0.913	0.931	0.874
				20	0.896	0.324	0.949	0.897
			1000	10	0.891	0.909	0.924	0.895
				20	0.919	0.926	0.914	0.916
		O_2	500	10	0.876	0.901	0.924	0.885
	343	Air	500	10	0.878	0.913	0.931	0.871
				20	0.948	0.960	0.968	0.945
			1000	10	0.977	0.987	0.983	0.978
		O_2	500	10	0.986	0.994	0.959	0.985
				20	0.983	0.986	0.959	0.982
			1000	10	0.979	0.985	0.917	0.964
				20	0.936	0.976	0.994	0.931
4.0	318	Air	750	15	0.868	0.883	0.877	0.863
					0.923	0.944	0.941	0.920
		O_2	750	15	0.987	0.995	0.984	0.985
	343	Air	750	15	0.984	0.975	0.935	0.983
					0.985	0.990	0.964	0.985
		O_2	330	15	0.928	0.715	0.557	0.953
			750	6.6	0.993	0.929	0.650	0.986
				15	0.997	0.960	0868	0.997
					0.982	0.979	0.976	0.962
					0.997	0.967	0.901	0.995
				23.4	0.990	0.886	0.534	0.992
			1170	15	0.983	0.862	0.697	0.978
4.5	318	Air	500	10	0.978	0.985	0.983	0.976
		O_2	500	10	0.983	0.865	0.741	0.993
	343	Air	500	10	0.916	0.772	0.664	0.919
				20	0.964	0.964	0.931	0.964
			1000	20	0.982	0.904	0.795	0.983
		O_2	500	10	0.954	0.802	0.669	0.971
				20	0.984	0.881	0.736	0.992
			1000	10	0.985	0.859	0.772	0.996
				20	0.987	0.860	0.737	0.996
4.8	343	O_2	750	15	0.987	0.860	0.737	0.996

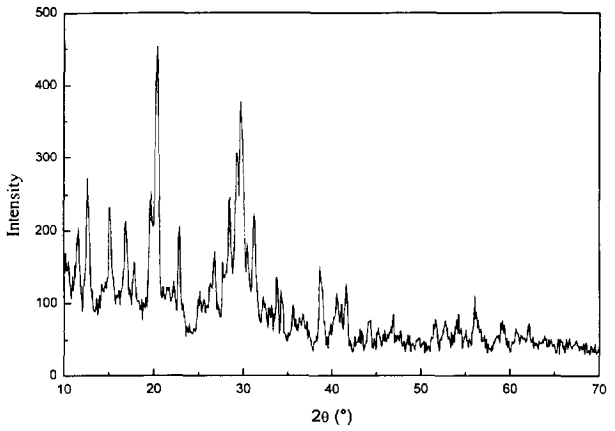

Fig. 11. XRD pattern of the product obtained at pH 3.0, $N=750$ rpm, $Q_o=10$ l min and $T=343$ K.

for the synthesis of magnetite is nucleated from G.C. II. This mechanism was confirmed by periodic sampling: all samples were a mixture of α-FeOOH and magnetite, with the same approximate ratio between the two compounds until the end of the experiment. This ratio varies as a function of the experimental conditions. $Fe(OH)_2$ was not observed in the mixtures. This confirms that magnetite is not formed previous to goethite and is not nucleated from precipitated ferrous hydroxide, suggesting its formation from G.C. II. This mechanism explains the competing behaviour observed in previous experiments.

At pH 6.5 or pH 6.8, when the temperature is fixed at 318 K, the mechanism must occur by the formation of G.C. II, because $Fe(OH)_2$ was not detected during sampling.

The correlations obtained during the kinetic study also confirm this mechanism. At the highest temperature and pH $\geq$ 5.5, the process shows shared control, with a slight trend to diffusion control, which is related to the formation of an intermediate solid. For the other experimental conditions, a second-order reaction controls the process, suggesting that more than one intermediate is involved.

A scheme of the overall mechanism is shown in Fig. 13.

The most important variable is the pH, which is responsible for the type of process which occurs and therefore for the

Table 8
Correlation indices for chemical reaction of order one, two or three with respect to Fe(II) and diffusion of O_2. Magnetite synthesis range

pH	T (K)	Oxidizer	N (rpm)	Q (l/min)	$m=1$	$m=2$	$m=3$	Diffusion
5.2	343	Air	625	7.5	0.948	0.776	0.487	0.955
5.5	343	Air	250	5	0.938	0.750	0.504	0.949
				10	0.984	0.792	0.484	0.990
			1000	5	0.939	0.726	0.646	0.950
				10	0.931	0.753	0.578	0.938
6.0	343	Air	0	7.5	0.910	0.742	0.520	0.915
			625	3.3	0.935	0.747	0.517	0.942
				7.5	0.945	0.807	0.614	0.964
					0.982	0.914	0.617	0.983
				11.7	0.911	0.748	0.619	0.916
			1255	7.5	0.973	0.892	0.608	0.974
6.5	318	Air	250	5	0.958	0.997	0.931	0.955
				10	0.951	0.987	0.934	0.947
			1000	5	0.998	0.945	0.847	0.996
				10	0.968	0.989	0.921	0.959
	343	Air	250	5	0.930	0.845	0.586	0.949
				10	0.897	0.714	0.523	0.907
			1000	5	0.966	0.834	0.572	0.950
				10	0.990	0.915	0.546	0.992
6.8	318	Air	750	7.5	0.945	0.972	0.877	0.933
	343	Air	750	7.5	0.969	0.889	0.721	0.621

Table 9
Kinetic constants for first-order reactions in the goethite synthesis range

pH	T (K)	Oxidizer	N (rpm)	Q (l/min)	$K \cdot 10^3$ (1/atm min)
4.0	318	O_2	750	15	1.16
	343	Air	750	15	5.97
					5.71
		O_2	330	15	2.54
			750	6.6	7.36
				15	3.25
					3.25
					2.99
				23.4	7.48
			1170	15	4.63
4.5	318	Air	500	10	5.91
		O_2	500	10	2.99
	343	Air	500	10	11.20
				20	4.78
			1000	20	7.35
		O_2	500	10	4.83
				20	6.02
			1000	10	2.01
				20	1.93
4.8	343	O_2	750	15	14.51

phase obtained. Only at intermediate pH values (pH 7 at 298 K, pH 6 at 318 K and pH 5 at 343 K), do the rest of the variables influence the development of one of the two processes. However, increasing temperature improves the speed of the reaction and promotes the synthesis of magnetite.

7. Conclusions

The elimination of Fe(II) by oxyprecipitation is kinetically controlled by a second-order or higher reaction at pH < 4, but with increasing pH, the control is shared by diffusion

Table 10
Kinetic constants for first-order reactions in the magnetite synthesis range

pH	T (K)	Oxidizer	N (rpm)	Q (l/min)	$K \cdot 10^2$ (1/atm min)
5.2	343	Air	625	7.5	2.11
5.5	343	Air	250	5	2.28
				10	2.37
			1000	5	3.54
				10	3.51
6.0	343	Air	0	7.5	2.97
			625	3.3	2.63
				7.5	5.19
					4.09
				11.7	3.33
			1255	7.5	3.75
6.5	343	Air	250	5	2.28
				10	3.06
			1000	5	3.54
				10	2.96
	343	Air	750	7.5	8.72

Fig. 12. Micrographs of products synthesized at $T = 343$ K, $N = 750$ rpm, $Q_0 = 10$ l min^{-1} and pH 3 (a), pH 4 (b), and pH 4.5 (c).

processes and a first-order reaction. In the higher pH range, at 318 K, a second-order reaction is the controlling stage. At 343 K, control is again shared by diffusion processes and a first-order reaction.

The proposed reaction mechanism is summarized in Fig. 13. The reactions produced as a function of pH at 343 K are as follows: (1) Goethite is obtained in a three-step process: G.C. II is nucleated, G.R. II is formed from the latter

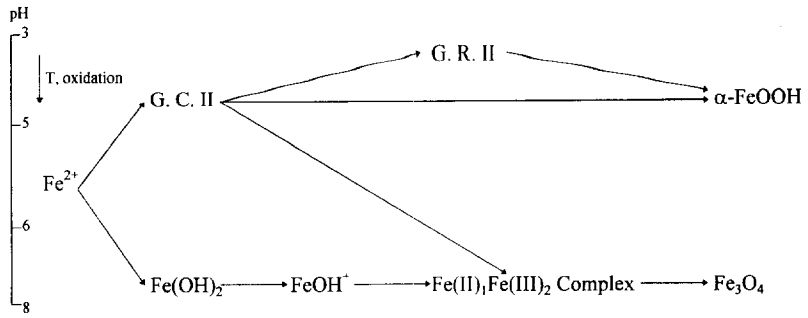

Fig. 13. Proposed reaction mechanism.

complex and, finally, goethite is precipitated. (2) Goethite is precipitated directly from G.C. II. (3) Magnetite is formed from a three-step mechanism: formation of G.C. II, nucleation of a complex with the same Fe(II)/Fe(III) ratio as magnetite and precipitation of the oxide. (4) $Fe(OH)_2$ is precipitated, followed by its redissolution as $FeOH^+$; the complex mentioned in (3) is formed from $FeOH^+$ and precipitates as magnetite.

8. List of symbols

$C_{Fe(II)0}$	initial Fe(II) concentration of pickling liquor (mol l^{-1})
$C_{Fe(II)}$	Fe(II) concentration of pickling liquor (mol l^{-1})
$Cm_{Fe(II)0}$	initial Fe(II) concentration of the tested pickling liquor (g l^{-1})
$Cm_{Fe(II)f}$	final Fe(II) concentration after oxyprecipitation process (g l^{-1})
$Cm_{Fe(III)f}$	final Fe(III) concentration after oxy-precipitation process (g l^{-1})
$D_{Fe(II)}$	diffusion coefficient of Fe(II)
D_{O_2}	diffusion coefficient of O_2
G.C. II	green complex II
G.R. II	green rust II
H_{O_2}	Henry's law constant
K	kinetic constant
K_{O_2g}	mass transfer coefficient in gas phase for oxygen
K_{O_2l}	mass transfer coefficient in liquid phase for oxygen
m	reaction order with respect to Fe(II)
n	reaction order with respect to O_2
N	stirring speed (rpm)
p_{O_2}	partial pressure of oxygen (atm)
Q	flow of oxidizer (l min^{-1})
Q_a	flow of air (l min^{-1})
Q_o	flow of oxygen (l min^{-1})
S	interfacial surface (cm^2)
t	time (min)
T	temperature (K)
Fe_{el} (%)	Fe(II) elimination rate $((Cm_{Fe(II)}/Cm_{Fe(II)0}) \times 100)$

References

[1] C. Negro, R. Latorre, J. Dufour, A, Formoso, F. López, J. Environ. Sci. Health A, 29 (1994) 1899–1926.
[2] L. Marabelli, A. Pini, Not. Ecol. 4 (8) (1986) 16–18.
[3] R. Rituper, Iron compounds, Ullmann's Encyclopedia of Industrial Chemistry, VCH, Weinheim, 5th edn. A14, 1990, pp. 604–605.
[4] W.K. Munns, Iron removal from pickle liquors using absorption resin technology, in: Iron Control Hydrometallurgy, Ellis Horwood, Chichester, 1986, pp. 537–548.
[5] J.C. McArdle, Iron Steel Eng. 68 (5) (1991) 39–43.
[6] H.M. Ismail, N.E. Fouad, M.I. Zaki, M.N. Nagar, Powder Tech. 63 (1990) 87–96.
[7] S. Yu, W. Zhichun, C. Chia-Yung, Iron removal for sulphuric acid solutions by solvent extraction mixtures of extractans, in: Iron Control Hydrometallurgy, Ellis Horwood, Chichester, 1986, pp. 335–351.
[8] F. López, F.J. García, A. Rubio, E. Sainz, R. Gancedo, J.F. Marco, Obtención de α-Fe_2O_3 mediante biooxidación de soluciones residuales de sulfato ferroso, Proc. IV Reunión Nacional de Materiales, Oviedo, Spain, 1993, pp. 73–74.
[9] T. Misawa, K. Hashimoto, S. Shimodaira, Corr. Sci. 14 (1974) 131–149.
[10] M. Kiyama, Bull. Chem. Soc. Japan 47 (1974) 1646–1650.
[11] E. Sada, H. Kumazawa, H.M. Cho, Can. J. Chem. Eng. 68 (1990) 622–626.
[12] T. Misawa, K. Hashimoto, S. Shimodaira, J. Inorg. Nucl. Chem. 35 (1973) 4167–4174.
[13] Y. Tamaura, T. Yoshida, T. Katsure, Bull. Chem. Soc. Japan 57 (1984) 2417–2421.
[14] J. Detournay, L. de Miranda, R. Derie, M. Ghodsi, Corr. Sci. 15 (1975) 295–306.
[15] A.A. Olowe, J.M.R. Genin, Ph. Bauer, Hyperfine Interact. 41 (1988) 501–504.
[16] Y. Tamaura, M. Saturno, K. Yamada, T. Katsura, Bull. Chem. Soc. Japan. 57 (1984) 2417–2421.
[17] A.A. Olowe, D. Rezel, J.M.R. Genin, Hyperfine Interact. 46 (1989) 429–436.

[18] J. Dufour, L. López, A. Formoso, C. Negro, R. Latorre, F. López-Mateos, Chem. Eng. J. 59 (3) (1995) 287–291.
[19] M. Kiyama, T. Takada, Bull. Chem. Soc. Japan 45 (1972) 1923–1924.
[20] J. Subrt, A. Solcova, F. Hanousek, A. Petrina, V. Zapletal, Coll. Czech. Comm. 49 (1984) 2478–2485.
[21] E. Sada, H. Kumazawa, H.M. Cho, Chem. Eng. Comm. 95 (1990) 145–151.
[22] J. Dufour, L. López, C. Negro, R. Latorre, F. López, A. Formoso, Optimización de la síntesis de magnetita por oxidación de disoluciones acuosas, Proc. IV Reunión Nacional de Materiales, Oviedo, Spain, 1994, pp. 360–361.